Static Nuclear Polarisation and Polarised Targets

W. Heeringa
Institut für Kernphysik

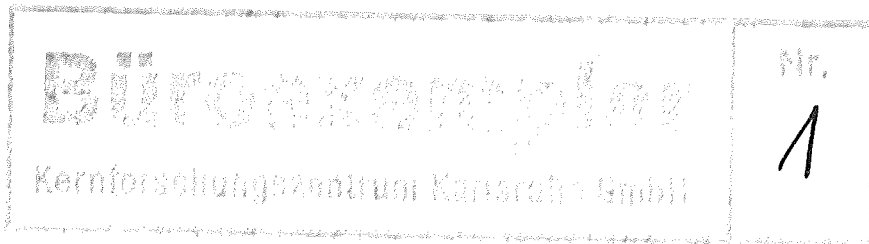**Kernforschungszentrum Karlsruhe**

KERNFORSCHUNGSZENTRUM KARLSRUHE

Institut für Kernphysik

KfK 3851

STATIC NUCLEAR POLARISATION AND POLARISED TARGETS

von

Wabe Heeringa

Kernforschungszentrum Karlsruhe GmbH, Karlsruhe

ABSTRACT

Recent progress and status of statically polarised
nuclear targets are reviewed. Special attention is
given to polarised ^{1}H and ^{3}He. An important quantity
in the determination of the target polarisation is the
thermal gradient over the target sample. The dependence
of this gradient on heat input, sample geometry, and
thermal conductivity of the sample is discussed. Possi-
bilities of performing experiments with proton beams
are indicated.

ZUSAMMENFASSUNG

Es wird ein Überblick über Stand und neueste Fortschritte
statisch polarisierter Targets für kernphysikalische Streu-
experimente gegeben. Besondere Aufmerksamkeit wird po-
larisiertem ^{1}H und ^{3}He gewidmet. Eine wichtige Größe für
die Bestimmung der Targetpolarisation ist der thermische
Gradient über die Targetprobe. Die Abhängigkeit des Gra-
dienten von Wärmefluß, Targetgeometrie und spezifischer
Wärmeleitfähigkeit des Probenmaterials wird diskutiert.
Möglichkeiten der Durchführung von Experimenten mit Pro-
tonenstrahlen werden angegeben.

CONTENTS

1. INTRODUCTION

In static nuclear polarisation the nuclei are in thermal equilibrium with their surroundings. The unequal population of the magnetic substates is brought about by the direct interaction of the nuclear magnetic moments with the magnetic field present at the nuclei. This is contrary to dynamic polarisation methods in which the nuclear polarisation is achieved by a mechanism which transfers an electronic polarisation to the nuclei. For static nuclear polarisation very low temperatures and high magnetic fields are necessary. For example, the static polarisation of protons at B = 10 T and T = 10 mK is P = 77%. The polarisation P is a function of the ratio of the magnetic field B and the temperature T:

$$P = \frac{2I+1}{2I} \coth \left(\frac{2I+1}{2} \frac{\mu B}{kT}\right) - \frac{1}{2I} \coth \left(\frac{\mu B}{2IkT}\right), \quad (1)$$

in which I and μ are the nuclear spin and magnetic moment, respectively, and k is the Boltzmann constant.

The large magnetic field, necessary for static polarisation can be provided in two ways. First, by an external magnet; this is called brute-force polarisation. Second, by a hyperfine field, which is created at the nuclei by unpaired electrons; this we shall call hyperfine polarisation. With the hyperfine polarisation method in general higher polarisations can be achieved than with the brute-force method, because the hyperfine fields are very high. They range from about 20 T for Co to 900 T for Ho, whereas the magnetic fields produced by an external magnet are in practical cases limited to about 10 T. The hyperfine polarisation method is widely applied to orient very small concentrations of all kinds of nuclides in magnetic host lattices. For polarised targets,

however, high concentrations of the nuclides to be studied are necessary. In this case the hyperfine method is limited to the magnetic elements themselves and to simple magnetic compounds. Rare earth metals have a complicated magnetic structure in most cases and therefore are hard to saturate magnetically. Often quite large external fields are applied to obtain a saturation as high as possible.

Table 1:

Brute-force polarisation of some isotopes calculated at T = 10 mK and B = 10 T. For ^{3}He a correction due to exchange interactions was applied.

Isotope	Polarisation (%)	Isotope	Polarisation (%)
^{1}H	77.0	^{63}Cu	41.8
^{2}H	20.6	^{65}Cu	44.3
^{3}He	54.6		
^{7}Li	56.6	^{93}Nb	67.4
^{9}Be	23.4	^{113,115}In	63.4
^{11}B	48.9	^{181}Ta	34.9
^{27}Al	53.4	^{185,187}Re	48.4
^{45}Sc	60.0	^{203,205}Tl	53.4
^{51}V	63.1	^{209}Bi	53.7
^{55}Mn	51.3		

The brute-force polarisation calculated for some nuclides at T = 10 mK and B = 10 T is listed in table 1. In table 2 the hyperfine fields of some magnetic elements and compounds are shown, which have been used already as po-

larised targets in an experiment. A complete reference
list of papers pertinent to the field of static nuclear
orientation up to June 1983 can be found in ref.1.

Table 2:

Hyperfine fields of some elements and compounds. As for
the compounds the field quoted is that of the under-
ligned element.

Element	$B_{hf}(T)$	Compound	$B_{hf}(T)$
Co	22	BiMn	~ 100
Tb	300	AuFe	145
Ho	900	US	330
Er	620	PrAl$_2$	170
Gd	35		
Dy	520		

2. MAGNETS AND REFRIGERATORS

The usefulness of a polarised target depends strongly
on the size of the magnetic field and the cooling power
of the refrigerator. The progress in magnet technology
for polarised targets is rather slow. The employment of
the high critical field superconductor Nb_3Sn has become
quite general now, but in practical cases the magnetic
fields that can be achieved still are limited to about
10 T due to the large bore and gap generally required for
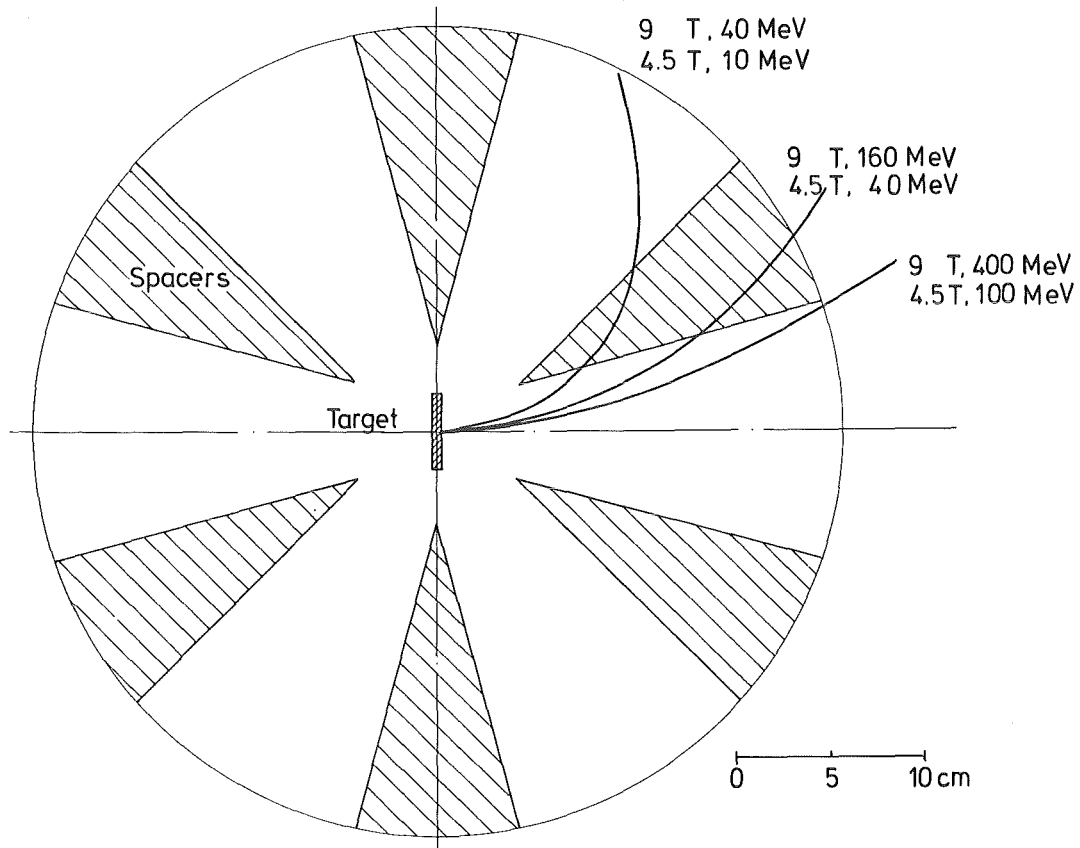nuclear physics experiments.

Fig.1: Calculated trajectories of proton beams through the polarising magnet of our institute run at 4.5 and 9 T.

Large magnetic fields imply an additional constraint on experiments with charged particles due to the bending of the beam in the magnetic field. Fig.1 shows, as an example, the trajectories of protons of different energies calculated for the 9 T polarising magnet (which, by the way, was designed for neutron experiments) of our institute. It appears that the large spacers, necessary in such a high field magnet, and the small radius of curvature prevent the free transmission of proton beams up to 400 MeV. If this magnet is run at 4.5 T, the same trajec-

tories would be followed by particles of four times
lower energies. Moreover, a magnet specially designed
for 4.5 T could have a smaller diameter and smaller
spacers, allowing possibly for proton experiments down
to 25 MeV. In experiments with hyperfine polarised tar-
gets, in which usually much lower fields are sufficient,
proton experiments down to 10 MeV and below are feasible.

As for dilution refrigerators, here a steady increase
in cooling power can be observed. The latest break-through
concerning dilution units designed for the low mK region
has been made by Frossati in 1977, who introduced the use
of very fine grain sintered silver powders in semi-con-
tinuous heat exchangers |2|. Larger cooling powers can be
obtained by building larger scale dilution units and employ-
ing them at a larger circulation rate. The limits are main-
ly set by the price of the pumping system, of the ^{3}He gas
and of the silver powder. The cooling power range of the
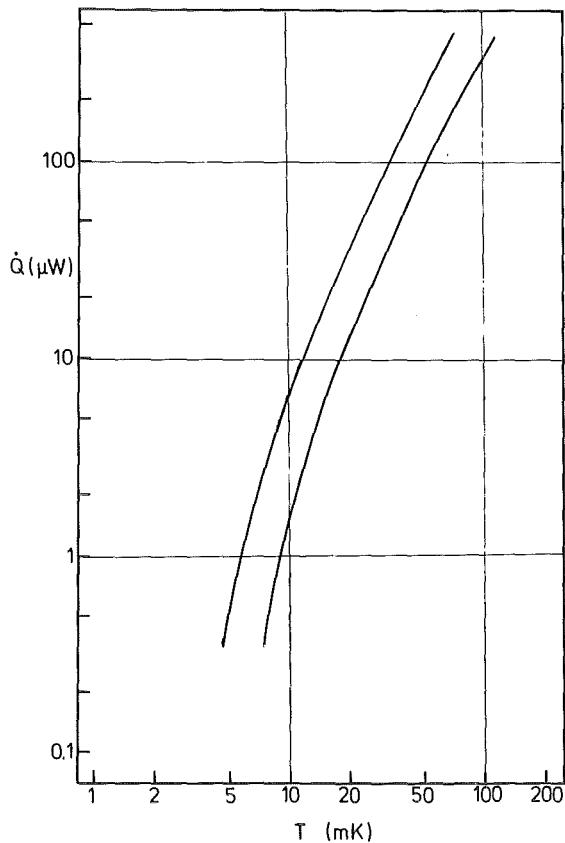most powerful dilution refrigerators commercially available
now is shown in fig.2.

Fig.2: Cooling power range
of the most powerful
dilution refrigera-
tors commercially
available at present.

An attractive alternative for the attainment of temperatures below 10 mK is the demagnetization of enhanced nuclear magnetic systems |3|. In such systems an external magnetic field induces an effective magnetic moment in the electron cloud, which in its turn induces a hyperfine field at the nucleus many times larger than the applied external field. Suitable materials are the intermetallic compounds $PrCu_6$ and $PrNi_5$. Precooling by a moderately powerful dilution refrigerator yields an appreciable cooling power at 5 mK and below. A 1.5 kg $PrCu_6$ sample (demagnetized from 3 T $\rightarrow$ 0.1 T, starting at 25 mK) can keep an other sample, with a heat load of 0.2 µW incident on it, below 4 mK for more than 40 hours |4|.

Such systems are employed in many laboratories now. At the research reactor in Petten a system with $PrNi_5$ is in operation, with which recently ^{23}Na, ^{47}Ti and ^{49}Ti have been polarised with the brute-force method for (n,γ) studies with polarised thermal neutrons |5,6|.

3. THERMAL GRADIENTS IN TARGET SAMPLES

3.1 General remarks

In thermal equilibrium the temperature attained by the nuclei of the polarised target depends on: 1) the cooling characteristics of the refrigerator, 2) the heat conductance of the connection to the target sample, 3) the geometry of the target, 4) the heat conductivity of the target material and 5) the heat load incident on the target.

Once the refrigerator is given, its cooling power is a fixed limit for any target construction connected to it.

The thermal conductance of the link between the target sample and the refrigerator should be sufficient when a rod or a bundle of wires of high purity copper or silver is used. Also the conductance between the sample and the thermal link should not pose a problem as long as metallic samples are employed.

In this section the problems concerning thermal contact between sample and refrigerator will not be considered. We shall concentrate on the last three topics mentioned above: target geometry, target conductivity and heat load. Low thermal conductivity in the sample itself may cause an unacceptable temperature gradient over it, even in cases where the heat load can easily be absorbed by the refrigerator. In order to be able to make some quantitative statements, we shall adopt a cylindrical shape of the sample, mounted into a ring shaped fitting. For thin targets, e.g. in the case of charged particle experiments, we shall also consider the case in which the target is mounted with its backside onto a substrate.

Let us first consider the case in which the target is cooled only by the ring shaped fitting at its outer diameter. The heat conductivity κ of the sample is assumed to be linearly proportional to the temperature T: $\kappa = \lambda T$. At low temperatures this is very generally the case for metallic materials. Let the radius of the sample be R, its length be 1, and the radius of the projectile beam (hitting the sample centrally) be R_1, see fig.3.

The following relation can now be derived for the temperature T_r at some radius r inside the sample to the temperature T_R at its outer radius:

$$T_r^2 = T_R^2 + \frac{\dot{Q}}{2\pi\lambda 1} \left(1 - \frac{r^2}{R_1^2} + 2 \ln \frac{R}{R_1}\right). \qquad (2)$$
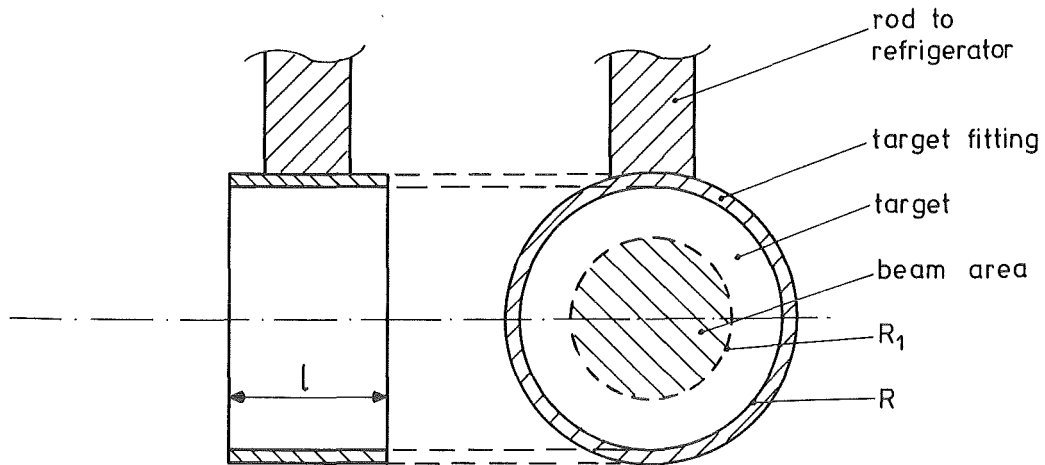
Fig.3: Target geometry for thermal gradient calculations.

Let us take for a numerical example a 1 cm thick Ti sample, and a heat load $\dot{Q}$ = 1 µW imposed by a beam with R_1 = R/2. Titanium has a rather poor heat conductivity with $\lambda \sim$ 0.25 W/K^{2}m. For T_R = 10 mK we find for the temperature at the centre of the sample T_0 = 16 mK. Hence, even for thick targets and moderate heat loads a substantial temperature gradient can occur due to low heat conductivity. The heat conductivity of several metallic materials at low temperatures is displayed in fig.4.
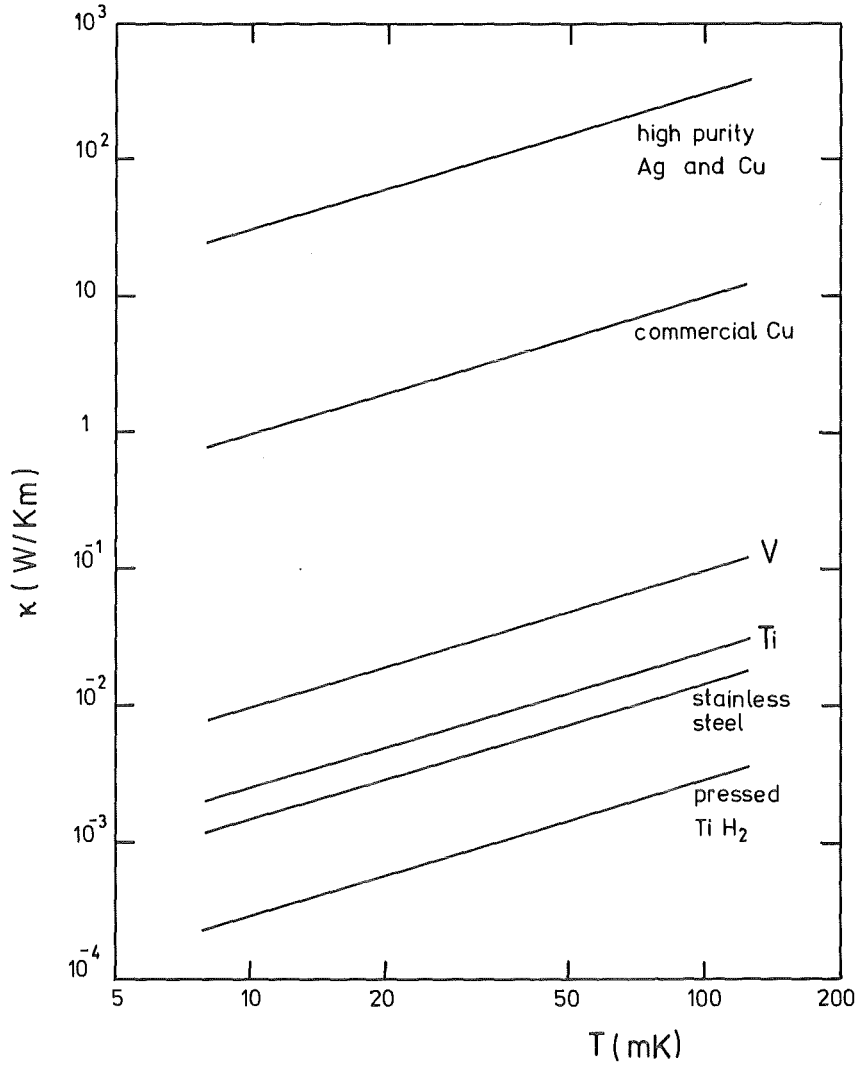
Fig.4: Heat conductivities of some metallic materials.

3.2 Neutron beams

Targets with a thickness of 1 cm or more are normally used in neutron experiments because of the low intensity of neutron beams. From an experimental point of view thick targets are allowed, because the direct neutron beam does not lose energy during passage through matter as opposed to charged particles. This is also advantageous from a cryogenic point of view.

The energy deposited by a neutron beam depends on its intensity, on the neutron energy and the target nuclides. Many nuclides have large neutron capture cross sections around thermal neutron energy. This leads to a large heat load due to β-radiation if the ground state of the compound nucleus is β-unstable, because the end-point energy of β-rays usually is some MeV. The heat load imposed by a thermal neutron beam with intensity 10^8 n s^{-1} on a 1 cm thick V target ($\sigma_{n,\gamma}$ = 5 b) is about 5 μW. The capture cross sections decrease at increasing energy, giving a much lower heat load in the keV-region and above. Above 1 MeV the capture cross section for ^{51}V is $\sigma_{n,\gamma}$ < 2mb, giving a heat load $\dot{Q}$ < 2 nW. Around 1 MeV the only important source of heat is the recoil energy absorbed by the nuclei in elastic scattering. At 1 MeV this yields a heat load in the 1 cm V target of about 20 nW with a beam of 10^8 n s^{-1}. This heat would increase linearly with energy (for nonrelativistic particles) for a constant total elastic cross section. The heat increases more at higher energies, where reaction channels open, in which charged particles are emitted. At 20 MeV the total cross section for charged particle emission is $\sigma_{n,c} \simeq$ 100 mb. Assuming that the charged particles will be stopped completely in the target we calculate a heat load of about 2 μW. This is of course a somewhat pessimistic assumption. To this heat the heat load of the vanadium recoils has to be added, which will be about 400 nW. Thus the total heat load may be expected to amount to 1 - 2 μW from a neutron beam with 10^8 n s^{-1}.

Resuming we find that a thermal neutron beam can deposit a large heat load due to neutron capture and subsequent β-decay. This varies strongly for different target nuclides due to the very large variations in thermal neutron capture cross section that are present over the periodic table. In the keV-region the heat load goes through a minimum. The subsequent increase in the MeV-region is

due to the increasing recoil energy at elastic scattering and to the opening of reaction channels emitting charged particles. The size of the heat load in the keV- and MeV-regions is quite similar for different nuclides.

3.3 Charged particle beams

Besides nuclear interactions charged particles interact with electrons by the Coulomb interaction on their way through matter. This gives rise to energy reduction and straggling and to angular straggling of a charged particle beam. Thin targets must be used in order to maintain an acceptable energy resolution.

Experiments with polarised targets and charged particle beams are very difficult due to this energy deposition. The energy loss is high for low energy particles, goes through a minimum for a kinetic energy around the rest mass of the particles and increases thereafter. From this point of view the optimal energy for experiments with polarised targets would be in the region of minimum ionisation, i.e. for protons around 1000 MeV, for example. In table 3 the energy loss of protons in a 0.1 mm V target is shown for increasing proton energies. Also shown is the heat input for a proton intensity of 10^8 protons/s (16 pA). We see that at 4 MeV the protons are still stopped completely in the target. At 20 MeV the energy loss of 1 MeV gives rise to an energy resolution of 5%, which may well be acceptable.

The heat input is 16 µW. The heat conductivity of V is moderate with $\lambda \sim 1.0$ W/K^2 m, see fig.4. Assuming a temperature $T_R = 10$ mK at the outer diameter of the target, we find for its temperature T_o at its centre: $T_o = 188$ mK (employing eq. (2) in which again $R_1 = R/2$ was taken). Thus polarisation of the target is impossible under these conditions. The most important reason for the high thermal

gradient in comparison with neutron experiments is the
fact, that the target has to be so much thinner, to keep
both the experimental resolution and the total heat in-
put low enough. The problems are less severe at higher
energy as is shown in table 3.

Table 3:

Energy-loss and heat input of a 16 pA proton beam
(10^8 protons/s) incident on a 0.1 mm thick V target.

E_p (MeV)	ΔE_p (MeV)	$\dot{Q}$ (μW)
4	4	64
10	1.9	30
20	1.0	16
100	0.3	5
1000	0.1	2

The thermal gradient will be much lower if the kind of
experiment to be carried out allows one to mount the tar-
get on a substrate of high-conductivity material of com-
parable or greater thickness. Instead of a radial gradient
we will then obtain a much lower axial temperature gradient.
Employing the same nomenclature as in section 3.1, one finds
for the temperature T_1 at the free side of the target

$$T_1^2 = T_0^2 + \frac{\dot{Q} \, l}{\pi R_1 \lambda}, \qquad (3)$$

where T_0 is the temperature of the substrate. With the num-
bers used above we obtain T_1 = 11 mK when T_0 = 10 mK in
the case of 20 MeV protons on the 0.1 mm V target (the ra-
dius of the beam has been taken to be R_1 = 5 mm). This is
an acceptable temperature gradient. Also the radial gra-
dient over the substrate can be kept low for a high-con-
ductivity substrate of sufficient thickness.

In fact this method of employing a substrate has been used for the only experiment of charged particle beams with statically polarised targets reported up to now |7|: the scattering of 10 MeV polarised protons from polarised ^{141}Pr and ^{165}Ho.

3.4 Comparison of neutron and proton experiments

Above we calculated a heat load of 2 μW on a 1 cm V target for a 20 MeV neutron beam with 10^8 n s^{-1}. A proton beam with the same intensity on a 0.01 cm thick V target imposes a heat input of 16 μW. Inspection of eq. (2) shows that the proton beam has to be lowered by a factor of 800 in intensity in order to obtain the same thermal gradient (T_O = 13 mK at T_R = 10 mK in a target without substrate). Thus for the same target polarisation, the neutron experiment has a luminosity which is a factor 800 (beam) x 100 (target) = 8 x 10^4 higher.

On the other hand, a neutron flux of 10^8 n s^{-1} is unrealistic in the MeV region. A realistic number is of the order of 10^3 - 10^5 n s^{-1}. With this flux the luminosities of the proton and the neutron experiment become of the same order of magnitude. Thus experiments with polarised targets and proton beams can be competitive with experiments with neutron beams already at 20 MeV and for moderately conducting targets. At higher energies and higher target conductivities the situation is even more advantageous for the proton beams. The main reason being, that neutron beams of only limited intensity are available in the MeV range. In general the experimental situation remains far below the cryogenic limits set by target conductivity and refrigerator cooling power. With charged particle beams one can always go close to these limits because any desired flux can easily be realised.

4. STATUS AND PROSPECTS OF EXPERIMENTS

4.1 Neutron beams

In the course of 30 years a large number of nuclides has been used as polarised targets in experiments with neutron beams at nuclear reactors. The main emphasis has been on transmission experiments for neutron resonance determinations and on (n,γ) spectroscopy experiments. A comprehensive review of this work has been given by Postma |8| recently. A continuous program is carried out in Petten employing polarised targets for (n,γ) work. Some recently polarized nuclides (brute-force method) are ^{23}Na |5|, ^{27}Al |9|, ^{47,49}Ti |6|, ^{51}V |10| and ^{63}Cu |11|. Occasionally heat load problems are encountered. The ^{51}V experiment suffered from an estimated heat load of 2 µW due to ß-radiation (see section 3.2), but generally the heat load is significantly lower. A large number of other isotopes can be studied with this method, especially because often only a small polarisation is required.

In the keV- and MeV-region transmission experiments have been carried out during the last decade with polarised neutrons and polarised targets to study the average neutron strength function difference (for $J = I +1/2$ and $J = I -1/2$ resonances) or the optical model spin-spin potential. Because the measured effects are small, large polarisations are needed. Therefore, up to now only hyperfine polarised targets have been employed, mostly ^{59}Co and ^{165}Ho, see e.g. refs. |12| and |13|. With the advent of more powerful refrigeration methods below 10 mK these experiments can now also be performed on many other nuclides, using brute-force polarisation. The heat input in such experiments is only small as we have seen in section 3.2. The neutron group in Durham has started such a program |14| for neutrons up to 20 MeV. The first nucleus they are investigating is ^{27}Al. First results are presented at this symposium |15|. Our

neutron group at the cyclotron in Karlsruhe has the
facilities to carry out such experiments from 20 -
50 MeV. The first experiment with this facility was
done during the last year employing a brute-force po-
larised proton target. This target is described in the
next chapter.

4.2 Charged particle beams

Experiments with charged particle beams and polarised
targets have only been reported by the group in Stanford,
who scattered about 10 MeV protons from polarised ^{141}Pr
and ^{165}Ho targets |7|. The target materials employed were
$PrAl_2$ and $HoAl_2$ with hyperfine fields of about 170 T and
460 T. The samples were magnetized by an external field
of 0.5 T. Very thin targets of about 1 μm were employed
in order to obtain a high enough energy resolution at this
low energy. These were mounted onto aluminum backings of
3 - 10 μm thickness. Proton currents of about 1 nA were em-
ployed, depositing a total heat load of the order of
100 μW in the target and the backing. The target tempera-
tures were estimated to be 160 mK and 125 mK with corres-
ponding polarisations of 56% and 83% for Pr and Ho, res-
pectively.

This experiment has shown that proton experiments down
to 10 MeV are feasible with hyperfine polarised targets.
For brute-force polarised targets a ten times lower tem-
perature and a ten times higher field are approximately
needed. In section 2 it was found that with a 4.5 T magnet
proton experiments will become practicable from about
25 MeV upwards. In section 3.4 it was argued that from the
point of view of thermal gradients proton experiments can
become competitive with neutron experiments from 20 MeV
upwards for targets without backing. If a backing can be
allowed, the thermal gradient will be smaller and higher
beam currents or thicker targets can be tolerated, yielding

higher count rates. Apart from this, experiments with protons offer a number of advantages over neutrons:

1. no limits in intensity

2. clean beams (MeV neutron beams usually consist of neutron groups of various energies)

3. always high beam polarisation possible

4. high and stable detection efficiency

5. high energy resolution (without the need of time-of-flight measurements).

We conclude that there seem to be real possibilities for experiments with brute-force polarised targets and proton beams below 100 MeV. In going to beams of heavier charged particles, experiments become less and less feasible due to the increasing stopping power at increasing charge and mass of the projectiles.

5. SPECIAL DEVELOPMENTS

5.1 Statically polarised protons

Polarised proton targets produced by the dynamic method are widely used in nuclear and high-energy physics. By the investment of large efforts in the past twenty years such targets have reached a high degree of performance, see for example ref. |16| and refs. therein. Besides this some effort has been spent in trying to develop a brute-force polarised proton target.

Pure solid H_2 would be the most desirable material. At low temperatures the H_2 molecules are in the para-state

(nuclear spins anti-parallel), making polarisation impossible. It is possible to freeze in a room temperature distribution with 75% ortho-hydrogen. However, the attainment of temperatures in the mK-range is made impossible by the heat released in the ortho-para conversion, which takes place at a finite rate. These problems are not present in HD molecules. Bozler et al. have obtained 40% proton polarisation in a 10 T field at 23 mK |17|.

A brute-force polarised proton target, which is easier to handle than HD has been developed recently in our institute |18|. It consists of pressed TiH_2 powder and has a length of 35 mm and a diameter of 25 mm. Its free proton density has the very high value of 9 x 10^{22} protons/ cm^3.

A polarisation of 60% has been measured for this target in a field of 8.2 T at a temperature around 12 mK. The measurement was carried out by transmitting 1.2 MeV polarised neutrons through the sample and determining the difference in count rate for parallel and anti-parallel spin orientations. This is a useful method because at low energies the neutron-proton spin-spin cross section is large and it is accurately known. Fig.5 shows the results of this experiment.

Besides the polarisation data from the transmission experiment also the temperature measurements of a ^{60}Co Co thermometer are shown, which was attached to the outside of the sample. The slight discrepancy between both data sets that remains towards the end of the experiment might be attributed to a small radial temperature gradient existing over the sample, or to a small systematic error in the quantities involved. The polarisation build-up time is several days. This is partly due to the poor heat conductivity of the pressed TiH_2 powder, which is shown in fig.4. The main reason, however, is the relatively low heat conductance

of the copper rod to the mixing chamber. This was kept
low deliberately in order to have an indication for the
heat flow through the rod. Thus considerably faster po-
larisation times are possible. The target is presently
being used in a scattering experiment with 20 - 50 MeV
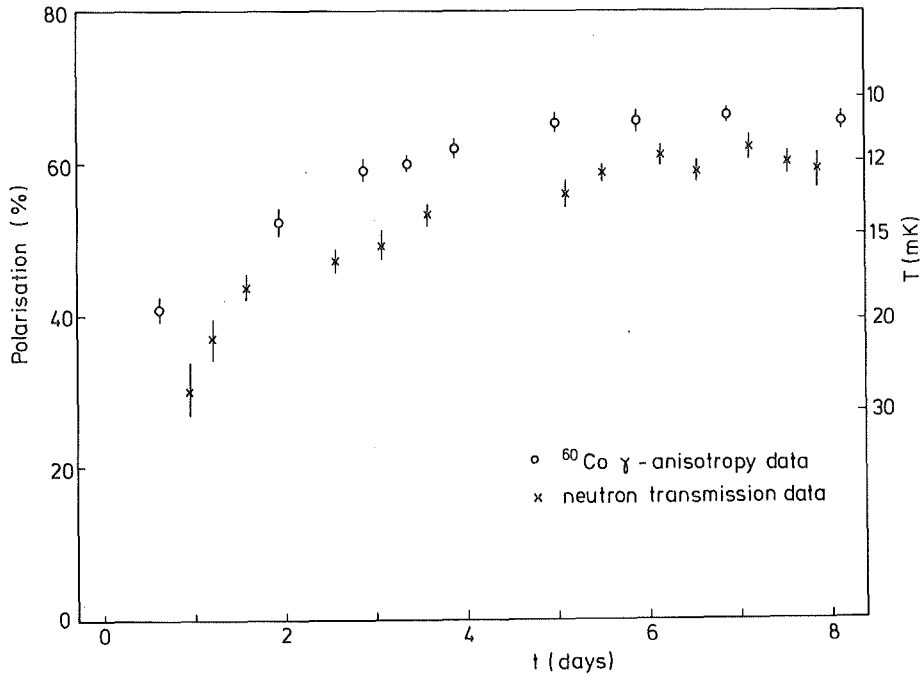polarised neutrons.

Fig.5: Results of the polarisation measurement of
protons in TiH_2.

An interesting development are the experiments present-
ly carried out in several laboratories with polarised atomic
hydrogen gas, see refs. |19| and |20|. The investigations
aim to reach such densities, that Bose-Einstein condensation
can be observed for this boson gas. The experiments are
carried out at high fields (~ 8 T) and low temperatures
(~ 250 mK). As a result the gas is initially electron-po-
larised, but not nuclear-polarised, the hyperfine-splitting
being of the order of 50 mK. The electron polarisation sta-

bilizes the atomic gas against recombination to H_2. The lowest hyperfine state can be written as $|a> = |\downarrow\uparrow> -\epsilon|\uparrow\downarrow>$, the other is a pure state: $|b> = |\downarrow\downarrow>$. The first arrow indicates the direction of the electron spin, the second the proton spin. The admixture ϵ of electron spin up is of the order of 10^{-3} at 8 T. Because of the finite value of ϵ atoms in state $|a>$ have a larger probability to recombine to H_2 than atoms in state $|b>$. Thus after a certain time the only atoms left are in state $|b>$ with 100% proton polarisation. Such a gas would of course present an ideal polarised proton target. Densities that are achievable continuously are of the order of $10^{17}/cm^3$ at present. The polarisation method is neither static nor dynamic, as defined in the beginning of this paper, but depends on the selective surrival of one hyperfine state through the recombination reaction.

5.2 Statically polarised ^3He

In order to cool and to polarise ^3He one can make use of a peculiar property of ^3He itself. This is the fact that on the melting curve of ^3He the molar entropy of solid ^3He is larger than that of liquid ^3He below 300 mK. Hence if a sample of liquid ^3He below this temperature is compressed so far that solidification sets in, this will be accompanied by a cooling of the ^3He. This adiabatic compressional cooling is known as Pomeranchuk cooling. Temperatures down to 2 mK can be obtained in starting from 50 mK or below. If the sample cell is placed in a strong magnetic field, the resulting solid ^3He will be polarised. The degree of polarisation can be calculated employing eq. (1) in which the magnetic field B has to be replaced by

$$B = B_{ext} - 3.85 \, P, \qquad (4)$$

where P is the polarisation and B_{ext} the externelly applied field. The correction is due to exchange interactions which

are important because of the large zero point motion of the ^{3}He atoms.

The cooling power of this method is given by

$$\dot{Q} = T (S_s - S_l)\dot{n}, \qquad (5)$$

where S_s and S_l are the entropies of the solid and the liquid and $\dot{n}$ is the conversion rate. For example, a heat load of 0.5 µW at a temperature of 10 mK will cause a solidification rate of about 1 cm^3/h.

This cooling method is a discontinuous process, ending when all liquid has been converted into solid. If only a low heat input is present, the polarisation can be maintained afterwards by the external cooling of a dilution refrigerator. The equilibrium polarisation is then also determined by the thermal conductivity of the solid ^{3}He and the Kapitza resis- tance between the solid and the connecting parts to the di- lution refrigerator.

A large number of Pomeranchuk cells are operating in the world nowadays, built to investigate the fascinating proper- ties of ^{3}He, see e.g. refs. |21| and |22|. A polarised ^{3}He target based on this method has not been constructed yet. A proposal for a feasibility study by Byckling et al. |23| appeared already in 1974.

6. CONCLUSIONS

Experiments with statically polarised targets have yielded valuable contributions to various fields of low-energy nuclear physics in the past thirty years. The steady improvements in magnet technology and new developments in refrigeration tech-

niques have opened the possibility of polarising more and
more different nuclides. With the increasing heat loads that
can be tolerated by the refrigerators the problem of thermal
gradients over the target samples becomes more important.
This is of course strongly dependent on the heat conductivi-
ty of the target material, which for different metallic samples
can vary up to five orders of magnitude.

In neutron experiments for which thick targets are used
thermal gradients can mostly be neglected. They can become
sizeable for poorly conducting targets with thermal neutron
beams (in the case of high (n,γ) cross sections) or with high
intensity beams in the higher MeV-region. In charged particle
experiments thermal gradients play a crucial role due to the
higher energy deposition and the smaller target thickness.
Other interfering factors are the total heat load to the re-
frigerator and the magnetic field. Because of this only one
experiment has been reported up to now with statically polarised
targets (hyperfine method) and proton beams. However, even ex-
periments with brute-force polarised targets and proton beams
are coming within reach now.

7. REFERENCES

| 1| 'Low Temperature Nuclear Orientation', ed. N.J. Stone
      and H. Postma (North-Holland, Amsterdam), in course of
      publication.

| 2| G. Frossati, J. de Phys. C6 (1978) 1578

| 3| B. Bleaney, Physica 69 (1973) 317

| 4| J.A. Konter, thesis, Leiden 1976

| 5| T.A.A. Tielens, thesis, Utrecht, 1983, to be publ. in
      Nucl. Phys.

| 6| J.F.A.G. Ruyl, thesis, Utrecht, 1983, to be publ. in
      Nucl. Phys.

| 7| J.H. Stanley, thesis, Stanford 1983

| 8| H. Postma in 'Low Temperature Nuclear Orientation',
      Ch.7, see ref. |1|

| 9| P.P.J. Delheij, A. Girgin, K. Abrahams, H. Postma and
      W.J. Huiskamp, Nucl. Phys. A341 (1980) 21

|10| J.B.M. de Haas, thesis, Leiden, 1979

|11| M.G. Delfini, J. Kopecky, J.B.M. de Haas, H.I. Liou,
      R.E. Chrien and P.M. Endt, Nucl. Phys. A404 (1983) 225

|12| W. Heeringa, H. Postma, H. Dobiasch, R. Fischer,
      H.O. Klages, R. Maschuw and B. Zeitnitz, Phys. Rev.
      C16 (1977) 1389

|13| U. Fasoli, G. Galeazzi, P. Pavan, D. Toniolo, G. Zago
      and R. Zannoni, Nucl. Phys. A311 (1978) 368

|14| C.R. Gould, D.G. Haase, T.B. Clegg, W.J. Thompson and
      R.L. Walter, Proc. 5th Intern. Symp. on Pol. Phen. in
      Nucl. Phys., Santa Fe, 1980, ed. G.G. Ohlsen, R.E. Brown,
      N. Jarmie, W.W. McNaughton and G.M. Hale (AIP Conf.
      Proceedings 69, 1981) p.944

|15| D.G. Haase, C.R. Gould and L.W. Seagondollar, contri-
      bution to this symposium

|16| W. Meyer, K.H. Althoff, W. Havenith, H. Riechert,
      E. Schilling and G. Sternal, Nucl. Instr. and Meth. 215
      (1983) 65

|17| H.M. Bozler, J.A. Brown and E.H. Graf, Bull. Am. Phys.
      Soc. 18 (1973) 545

|18| R. Aures, W. Heeringa, H.O. Klages, R. Maschuw, F.K. Schmidt
      and B. Zeitnitz, Nucl. Instr. and Meth. 224 (1984) 347

|19| R.W. Cline, T.J. Greytak and D. Kleppner, Phys. Rev.
      Lett. 47 (1981) 1195

|20| R. Sprik, J.T.M. Walraven, G.H. van Yperen and
     I.F. Silvera, Phys. Rev. Lett. 49 (1982) 153

|21| G. Schumacher, D. Thoulouze, B. Castaing, Y. Chabre,
     P. Segransen and J. Joffrin, J. de Phys. 40 (1979)
     L-143

|22| R.C.M. Dow and G.R. Pickett, Proc. 17th Int. Conf.
     on Low Temp. Phys., ed. U. Eckern, A. Schmid, W. Weber
     and H. Wühl (North-Holland, Amsterdam, 1984) p.557

|23| E. Byckling, O.V. Lounasmaa and T.O. Niinikoski,
     private communication, 1974